PHASE COMPOSITIONS IN ALLOY 718: A COMPARISON BETWEEN APT/APFIM MEASUREMENTS AND THERMODYNAMIC PREDICTIONS

M. K. Miller and S. S. Babu

Metals and Ceramics Division
Oak Ridge National Laboratory
P. O. Box 2008
Oak Ridge, TN 37831-6376

Abstract

Atom probe tomography has revealed that the individual secondary precipitates that form in Alloy 718 on low temperature annealing at 873 K are a mixture of the γ″ and γ′ phases. In addition, small γ′ precipitates were observed on the surface of the primary γ″ precipitates. The compositions of the γ, γ′ and γ″ phases have been determined experimentally by atom probe tomography and the results have been compared to thermodynamic predictions based on the Thermocalc™ program. The solute partitioning is in qualitative agreement with the thermodynamic predictions but quantitatively there are significant differences between the measured and predicted solute concentrations.

Introduction

In order to improve the properties of nickel-base superalloys, it is essential to determine the partitioning behavior of the solute additions within the microstructure. The techniques of atom probe field ion microscopy (APFIM) and atom probe tomography (APT) permit the solute partitioning and compositions of the coexisting phases to be determined with near atomic resolution [1,2]. These atom probe techniques are particularly powerful for the characterization of these complex superalloys due to the number of elements present and the fine scale of some of the features present in the microstructure.

Niobium-containing Alloy 718 is strengthened by a combination of DO_{22}-ordered γ″ and $L1_2$-ordered γ′ precipitates [3-7]. The crystal structures of both precipitates are derivatives of the face centered cubic structure and these precipitates have a cube-on-cube orientation relationship with each other and the γ matrix. The DO_{22}-ordered structure may be described as an $L1_2$-ordered structure with an $a[\frac{1}{2}\ \frac{1}{2}\ 0]$ displacement every other 001 plane thereby converting a cubic structure into a tetragonal one. The composition of both ordered phases can be described as $Ni_3(Al,Nb,Ti)$ with different levels of niobium, aluminum and titanium. However, it is advantageous to know the precise levels of all the elements in each phase so that the alloy composition can be optimized. In this paper, the results of an atom probe tomography characterization of the compositions of the coexisting phases are compared to thermodynamic predictions.

Previous atom probe field ion microscopy and transmission electron microscopy characterizations of this superalloy have demonstrated that the intragranular microstructure consists of the γ matrix at 1311 K. After annealing at 1143 K, lenticular DO_{22}-ordered γ″ precipitates are present in the γ matrix [3-7]. On further ageing at temperatures in the range 873 to 1033 K, small roughly spherical secondary precipitates form in the γ matrix. The precise identity of these secondary precipitates was not established experimentally until recent atom probe tomography studies were performed. Atom probe tomography revealed that the composition of the secondary precipitates were not uniform throughout their volume but divided into two distinct types of regions [8,9]. One of these regions was enriched in niobium and the other in aluminum and titanium. The compositions and crystal structures of these two types of regions are characteristic of the γ″ and γ′ phases, respectively. The interface between these regions was determined to be on the $(001)_{\gamma''}$ //$\{001\}_{\gamma'}$ planes.

A Laves (C14) phase with a composition consistent with $(NiCr_{0.5}Fe_{0.5})_2(NbMo)$, an orthorhombic δ ($Ni_3Nb$) phase and coarse MC carbides have also observed in Alloy 718 by transmission electron microscopy [6]. The Laves and δ phases were observed at grain boundaries and the MC carbide was observed both within the grains and occasionally at grain boundaries. No σ phase was observed in this previous transmission electron microscopy characterization [6].

Experimental

The composition of the Alloy 718 used in this investigation is given in Table I. All compositions quoted are in atomic percent. All specimens were given a treatment of 1 h at 1311 K (A) and some were given an additional treatment of 8 h at 1143 K (AC). These two stages are standard for a commercial heat treatment for these alloys. These two conditions were also investigated after subsequent isothermal ageing treatments at 873 K for times from 10 h up to 2012 h. The specimens were water quenched to room temperature between each stage.

The microstructure and compositions of the γ matrix as well as the γ″ and γ′ phases were determined experimentally with an energy-compensated three-dimensional atom probe [2]. Analyses were performed with a specimen temperature of between 50 and 60 K, a pulse fraction of 20% and a pulse repetition rate of 1500 Hz. Field ion micrographs were recorded with neon as the image gas and with a specimen temperature of 60 K. The chromium-enriched σ phase and the carbides were not characterized in this investigation due to their low volume fractions.

Thermodynamic predictions

The equilibrium compositions and the volume fractions of the phases at the different annealing temperatures were predicted with the Thermocalc™ program for three different temperatures, 1311, 1143 and 873 K based on the bulk composition of the alloy. The calculations describe multi-component and multi-phase thermodynamic equilibrium. The calculations used an 11 element Ni-Fe database [10]. The alloying elements considered in the calculations are Ni, Fe, Al, Nb, Ti, Cr, Co, Mo, and C. The phases considered in the equilibrium calculations are Ni_3Nb, MC carbonitride, γ (face centered cubic), γ′ ($L1_2$-ordered), σ, δ′, M_6C, laves, $M_{23}C_6$, M_7C_3, and liquid. The results are summarized in Table I. At 1311 K, this program predicts that the microstructure is predominantly γ matrix with small amounts of (Nb,Ti,Mo,Cr)C and $(Nb,Mo,Cr)_6C$ carbides. At 1143K, the γ matrix coexists with the Ni_3Nb phase and a minor amount of (Nb,Ti,Mo,Cr)C carbide. However, the $(Nb,Mo,Cr)_6C$ is not stable at this temperature. At 873K, the volume fraction of Ni_3Nb phase increases, and the γ′ and chromium-enriched σ phases are also present. In addition, the (Nb,Ti,Mo,Cr)C carbide is no longer stable at 873 K and is replaced with a chromium-rich $M_{23}C_6$ carbide.

Table I. Equilibrium compositions of the phases at the different annealing temperatures as predicted with the Thermocalc™ program. The balance of each analysis is nickel and the data are in atomic percent.

Phase	**Temp.**	**Cr**	**Fe**	**Nb**	**Mo**	**Ti**	**Al**	**Co**	**C**	**Moles**
Bulk	**K**	**21.80**	**20.30**	**3.20**	**1.81**	**1.15**	**0.96**	**0.26**	**0.26**	**%**
γ	1311	21.87	20.61	2.66	1.73	1.13	0.94	0.26	0.008	98.6
	1143	24.44	22.92	0.91	2.00	0.58	1.01	0.27	0.008	87.9
	873	23.73	26.38	0.09	1.13	0.05	0.25	0.26	-	70.7
γ′	873	0.54	2.70	5.94	0.09	8.07	9.50	0.11	-	7.5
Ni_3Nb	1143	1.05	1.56	19.62	0.49	4.59	0.30	0.17	-	11.6
	873	0.24	0.48	20.60	0.38	3.82	0.20	0.13	-	13.2
σ	873	53.80	19.24	-	11.45	-	-	0.46	-	7.2
MC	1311	0.06	-	35.87	0.13	17.67	-	-	46.27	0.2
	1143	0.04	-	32.43	1.06	20.52	-	-	46.90	0.5
M_6C	1311	3.69	0.08	44.96	8.23	-	-	-	14.29	1.2
$M_{23}C_6$	873	67.67	1.26	-	10.12	-	-	-	20.69	1.3

In addition to these predictions, a second set of thermodynamic predictions were performed for 873K that were based on the composition of the γ phase at 1143 K. This temperature defined the matrix composition from which the secondary precipitates formed. The results are summarized in Table IIa. A comparison of these two sets of predictions reveals some minor differences. Comparing the predictions for the γ concentrations at 873 K when starting with the γ composition at 1143 K versus the bulk composition reveals that the chromium, niobium and aluminum levels are slightly higher in the former predictions and the iron level is slightly lower. Similarly in the γ′ phase, the chromium, niobium, molybdenum and aluminum are slightly higher and the iron and titanium are slightly lower. In the Ni_3Nb phase, the niobium and aluminum are slightly higher and the chromium, iron, and titanium are slightly lower. The ratio of the volume fractions of the additional secondary γ′ and Ni_3Nb phases do not change significantly between these two calculations. The differences in the predicted compositions of the σ phase and the $M_{23}C_6$ carbide are extremely small.

These thermodynamic calculations were also performed with the suppression of the σ phase and the results are summarized in Table IIb. The suppression of the chromium- and molybdenum-enriched σ phase increases the amount of the γ phase and increases the chromium and molybdenum contents of the γ, γ′ and Ni_3Nb phases. Some minor changes were also observed in the other elements in these phases.

Table II. Equilibrium compositions of the phases at 873 K as predicted with the Thermocalc™ program based on the composition of the γ matrix at 1143 K: a) with σ phase, b) with σ phase suppressed. The balance of each analysis is nickel and the data are in atomic percent.

a) Phase	**Cr**	**Fe**	**Nb**	**Mo**	**Ti**	**Al**	**Co**	**C**	**Moles %**
γ at 1143 K	**24.44**	**22.92**	**0.91**	**2.00**	**0.58**	**1.01**	**0.27**	**0.008**	
γ	23.87	25.85	0.10	1.14	0.04	0.30	0.26	-	82.1
γ′	0.57	2.44	6.42	0.12	6.79	10.41	0.11	-	7.3
Ni_3Nb	0.22	0.44	21.41	0.39	2.91	0.29	0.12	-	1.7
σ	53.77	18.72	-	11.69	-	-	0.45	-	8.8
$M_{23}C_6$	67.72	1.22	-	10.01	-	-	-	20.69	0.01

b) Phase	**Cr**	**Fe**	**Nb**	**Mo**	**Ti**	**Al**	**Co**	**C**	**Moles %**
γ at 1143 K	**24.44**	**22.92**	**0.91**	**2.00**	**0.58**	**1.01**	**0.27**	**0.008**	
γ	26.89	25.00	0.07	2.17	0.03	0.26	0.28	-	91.0
γ′	0.61	2.27	6.47	0.18	6.87	10.56	0.11	-	7.2
Ni_3Nb	0.31	0.51	21.16	0.53	3.05	0.27	0.13	-	1.8
$M_{23}C_6$	67.88	1.05	-	10.18	-	-	-	20.69	0.01

Results and Discussion

A volume of atom probe tomography data containing an interface between a primary γ″ precipitate and the γ matrix in the material aged for 1 h at 1311 K, 8 h at 1143 K and 500 h at 873 K, is shown in Fig. 1. The phases observed in the atom probe were identified from their measured compositions and from correlation with the electron diffraction results of the previous transmission electron microscopy study [4-7]. The iron plus chromium isoconcentration surface delineates the interface between the primary γ″ precipitate and the γ matrix. In addition, the aluminum isoconcentration surface reveals the presence of two small γ′ precipitates on the surface of the primary γ″ precipitate. The composition of these γ′ precipitates was determined to be Ni-10.6±0.6 at. % Al, 10.5±0.6% Nb, 6.8±0.5% Ti, 2.1±0.3% Fe, 1.6±0.2% Cr. Concentration profiles normal to the γ″–γ interface, shown in Fig. 2a, reveal a marked ~1-nm-thick enrichment of niobium and depletions of chromium, iron and titanium on the γ″ side of the γ″–γ interface. Similarly, concentration profiles through a γ′ precipitate are shown in Fig. 2b. The partitioning of the aluminum, titanium and niobium to the γ′ precipitate is clearly evident. The morphologies of these ultrafine γ′ precipitates are oblate spheroids that are ~4 nm thick by ~10 nm diameter. These γ′ precipitates were not observed in the material after the preliminary 1 h at 1311 K and 8 h at 1143 K annealing treatment. This observation indicates that the γ′ precipitates formed during the 873 K anneal. A 1- to 2-nm-deep depression in the surface of the primary γ″ precipitate was observed under the γ′ precipitates. This depression suggests that the γ′ precipitate nucleates on the original surface of the primary γ″ precipitates

and then grows into the γ matrix. In addition, the primary γ″ precipitates coarsen by 1 to 2 nm during the 873 K annealing treatment.

The evolution of the size and morphology of the brightly-imaging secondary precipitates as a function of annealing time at 873 K is shown in Figs. 3 and 4. Some impingement of the secondary precipitates was observed after 10 h of ageing, as shown in Fig. 4a. The roughly spherical morphology of these secondary precipitates after 2012 h of ageing is also evident in the isoconcentration surfaces shown in Fig. 4b. The size of these secondary precipitates was found to follow a t^a power law where the time exponent a was 0.34. A decrease in the number density from 1.8 x 10^{25} to 9.1 x 10^{23} m^{-3} was observed between the 10 and 2012 h annealing times.

A composition profile through the central region of a secondary precipitate is shown in Fig. 5. The orientation of the composition profile is perpendicular to the (001) planes. Therefore, the compositions of the individual atomic planes are distinguished. The first thirteen planes are in the niobium-enriched γ″ phase and the remainder are in the aluminum-enriched γ′ phase. The ordering between the nickel (A) planes and the mixed B and C planes is clearly evident. The first mixed plane in the γ′ phase is significantly enriched in aluminum. This aluminum enrichment is also evident in the atom maps of the secondary precipitates and indicates rejection of aluminum from the γ″ phase.

The phase compositions of the γ matrix and the intragranular γ″ and γ′ phases, as determined by atom probe tomography, are presented in Table III. The compositions have been divided into two sections: one section from material annealed for 1 h at 1311 K and 2012 h at 873 K and a second section for material annealed for 1 h at 1311 K, 8 h at 1143 K and 2012 h at 873 K. In this table, the reported compositions are the averages of several measured regions. The individual composition determinations were performed by defining small volumes within the three-dimensional volume of analysis that contained only one specific phase and counting the number of atoms of each element within those volumes.

Atom probe composition measurements reveal that the γ matrix is characterized by high levels of chromium, iron and molybdenum and by low levels of niobium, titanium and aluminum. The γ″ phase is characterized by high levels of niobium and titanium and by low levels of chromium, iron and molybdenum. The γ′ phase is characterized by high levels of aluminum, titanium and niobium and by low levels of chromium, iron and molybdenum. The solute partitioning is in qualitative agreement with the thermodynamic predictions. However, there are some differences between the measured and predicted solute concentrations. The niobium and titanium levels measured in the γ matrix were significantly higher than predicted. The chromium level measured in the γ″ phase was also higher than predicted. The molybdenum levels measured in all phases were higher than predicted. Better agreement is found between the molybdenum level in the γ phase measured with the atom probe and the thermodynamic predictions when the σ phase was suppressed from the calculations. Some of the differences may also arise because the 2012 h aging time at 873 K may not be sufficient to reach equilibrium for all elements due to kinetic effects.

Table III. Compositions of the coexisting intragranular phases as determined by atom probe tomography. The balance of each analysis is nickel and the data are in atomic percent.

Aged 1 h at 1311 K + 2012 h at 873 K

Phase	**Time**	**Cr**	**Fe**	**Nb**	**Mo**	**Ti**	**Al**	**Co**
γ	2012 h	27.0 ± 0.36	26.2 ± 0.35	0.58 ± 0.05	2.26 ± 0.10	0.19 ± 0.03	0.22 ± 0.03	0.25 ± 0.03
γ′	2012 h	0.39 ± 0.07	1.78 ± 0.16	7.65 ± 0.33	0.76 ± 0.10	5.61 ± 0.28	9.46 ± 0.37	0.21 ± 0.06
γ″	2012 h	1.75 ± 0.31	1.29 ± 0.33	16.6 ± 1.19	1.56 ± 0.37	3.75 ± 0.57	0.43 ± 0.19	0.17 ± 0.12

Aged 1 h at 1311 K + 8 h at 1143 K + indicated time at 873 K

Phase	**Time**	**Cr**	**Fe**	**Nb**	**Mo**	**Ti**	**Al**	**Co**
γ	2012 h	23.8 ± 0.31	25.6 ± 0.33	0.52 ± 0.05	2.54 ± 0.10	0.13 ± 0.02	0.19 ± 0.03	0.38 ± 0.04
γ′	2012 h	0.59 ± 0.05	1.57 ± 0.24	8.21 ± 0.55	1.22 ± 0.21	7.30 ± 0.52	9.28 ± 0.58	0.30 ± 0.10
γ″	2012 h	1.98 ± 0.31	0.81 ± 0.20	20.6 ± 1.01	2.37 ± 0.34	3.68 ± 0.34	0.40 ± 0.14	0.20 ± 0.10
Primary γ″	500 h	2.00 ± 0.19	1.43 ± 0.16	16.0 ± 0.54	2.38 ± 0.21	5.68 ± 0.31	0.41 ± 0.09	0.39 ± 0.08

Conclusions

Atom probe tomography has revealed that the secondary precipitates that form in Alloy 718 during low temperature annealing at 873 K are a mixture of the γ″ and γ′ phases. In addition, small γ′ precipitates were observed on the surface of the primary γ″ precipitates. The solute partitioning is in quantitative agreement with thermodynamic predictions but there are some significant differences between the measured and predicted solute concentrations.

Acknowledgements

The author would like to thank K. F. Russell of Oak Ridge National Laboratory and Dr. M. G. Burke of Bechtel Bettis, Inc., West Mifflin, PA for their assistance. This research was sponsored by the Division of Materials Sciences, U. S. Department of Energy, under contract DE-AC05-96OR22464 with Lockheed Martin Energy Research Corp. This research was conducted utilizing the Shared Research Equipment (SHaRE) User Program facilities at Oak Ridge National Laboratory.

References

1. M. K. Miller, A. Cerezo, M. G. Hetherington and G. D. W. Smith, Atom Probe Field Ion Microscopy (Oxford, England: Oxford University Press, 1996).

2. M. K. Miller, “Three-dimensional atom probes,” J. Microsc., 186 (1997), 1-16.
3. Proc. Superalloy 718, June 1989, Pittsburgh PA, ed. E.A. Loria (Warrendale, PA: The Minerals, Metals and Materials Society, 1989).
4. M. G. Burke and M. K. Miller, “APFIM/TEM characterization of precipitation in Alloy 718,” J. de Physique, 50-C8 (1989), 395-400.
5. M. K. Miller and M. G. Burke, “ Atom probe analysis of the compositions of γ′ and γ″ intermetallic phases in nickel-based superalloy 718,” Proc. Alloy Phase Stability and Design, April 1990, San Francisco, CA, vol. 186, eds., G. M. Stocks, S. P. Pope and A. F. Giamei (Pittsburgh, PA: Materials Research Society 1991), 223-228.
6. M. G. Burke and M. K. Miller, “Grain boundary intermetallic phases in Alloy 718,” Proc. Alloy Phase Stability and Design, April 1990, San Francisco, CA, vol. 186, eds., G. M. Stocks, S. P. Pope and A. F. Giamei (Pittsburgh, PA: Materials Research Society 1991), 215-218.
7. M. G. Burke and M. K. Miller, “Precipitation in Alloy 718: A combined AEM and APFIM investigation,” Proc. Superalloys 718, 625 and Various Derivatives, June 1991, Pittsburgh, PA, ed. E. A. Loria, (Warrendale, PA: The Minerals, Metals and Materials Society, 1991) 337-350.
8. M. K. Miller, S. S. Babu and M. G. Burke, “Intragranular precipitation in Alloy 718,” Mater. Sci. Eng., A270 (1999), 14-18.
9. M. K. Miller, “Atom probe studies of phase transformations in nickel-based superalloys,” Proc. Int. Conf. Solid-Solid Phase Transformations PTM’99, Kyoto, Japan, May 1999, eds. M. Koiwa, K. Otsuka and T. Miyazaki, (Sendai, Japan: The Japan Institute of Metals, 1999) in press.
10. N. Saunders, "Ni-data information", Thermotech Ltd., Surrey Technology Center, Guildford, Surrey, GU2 5YG, UK.

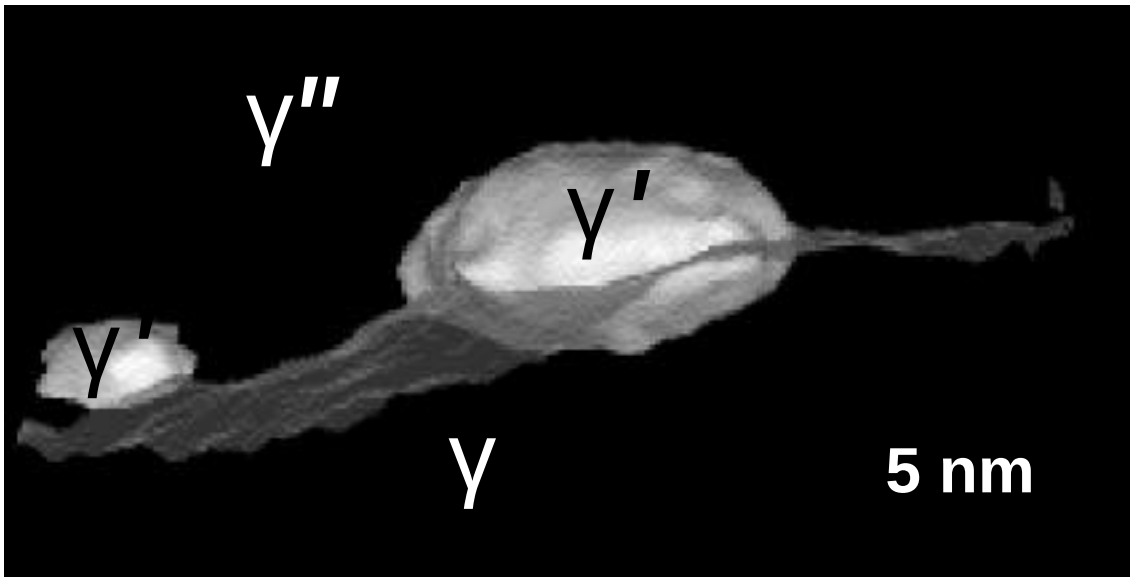

Fig. 1. Iron plus chromium isoconcentration surface delineating the surface of a primary γ″ precipitate and alumimum isoconcentration surfaces delineating two secondary γ′ precipitates in Alloy 718 aged for 1 h at 1311 K, 8 h at 1143 K and 500 h at 873 K.

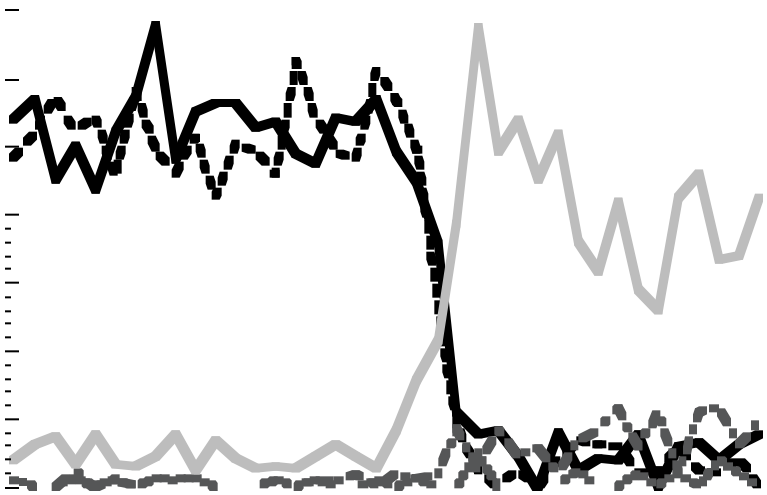

Fig. 2. Concentration profiles a) from the γ matrix into a primary γ″ precipitate and b) from the γ matrix through a γ′ precipitate into a primary γ″ precipitate in Alloy 718 aged for 1 h at 1311 K, 8 h at 1143 K and 500 h at 873 K.

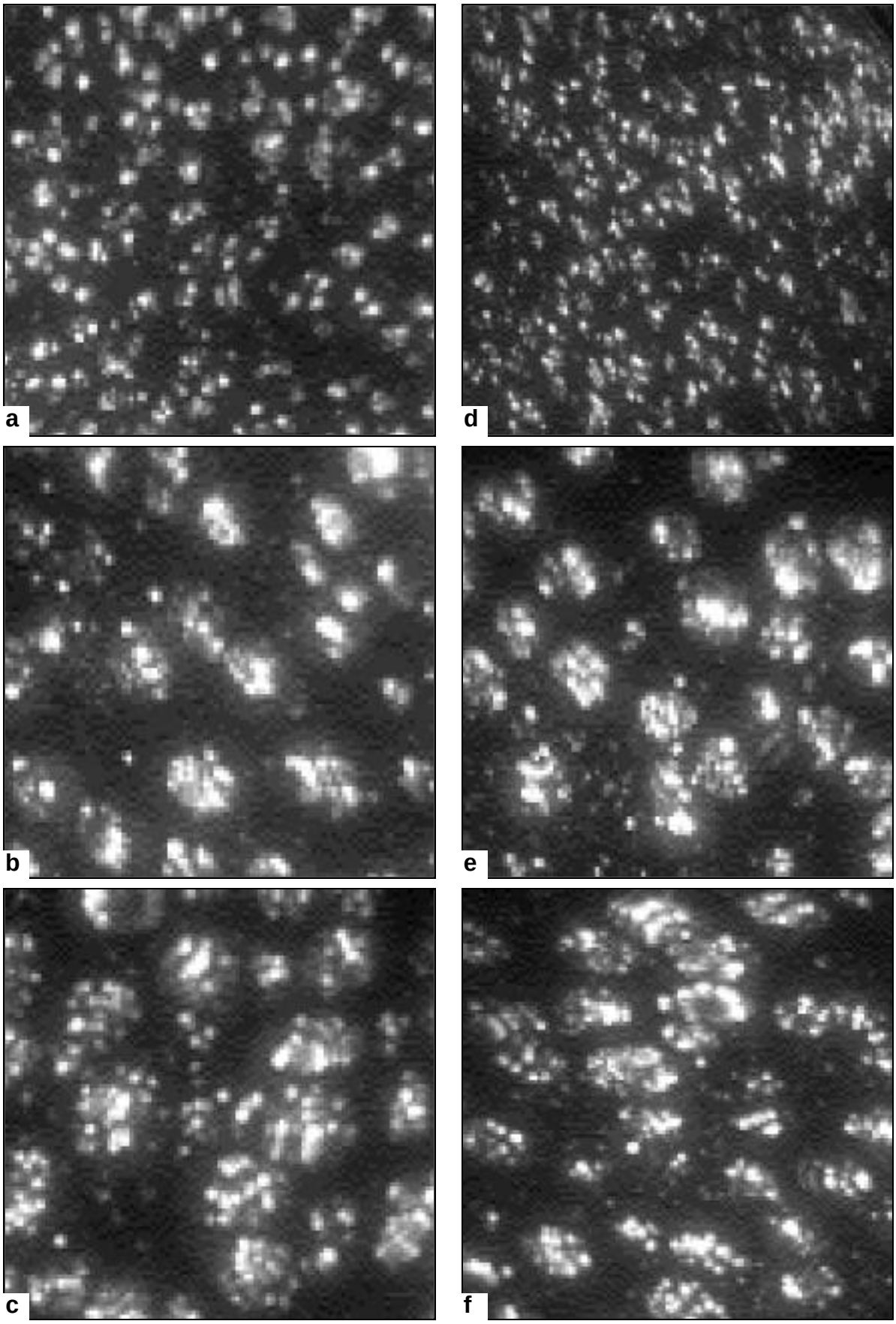

Fig. 3. Field ion micrographs of the brightly-imaging secondary precipitates in Alloy 718 aged for 1 h at 1311 K + a) 100 h, b) 500 h and c) 2012 h at 873 K and 1 h at 1311 K, 8 h at 1143 K + d) 100 h, e) 500 h and f) 2012 h at 873 K.

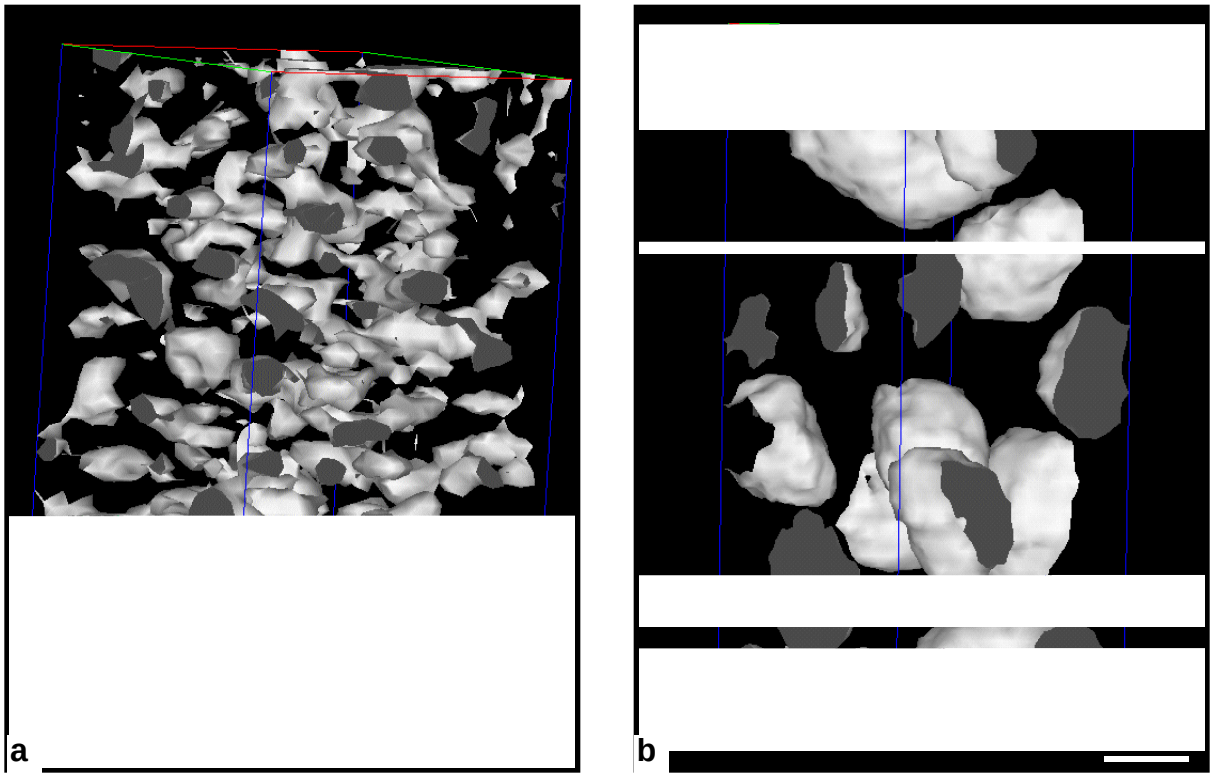

Fig. 4. Iron plus chromium isoconcentration surfaces delineating the secondary precipitates in Alloy 718 aged for 1 h at 1311 K + a) 10 h and b) 2012 h at 873 K.

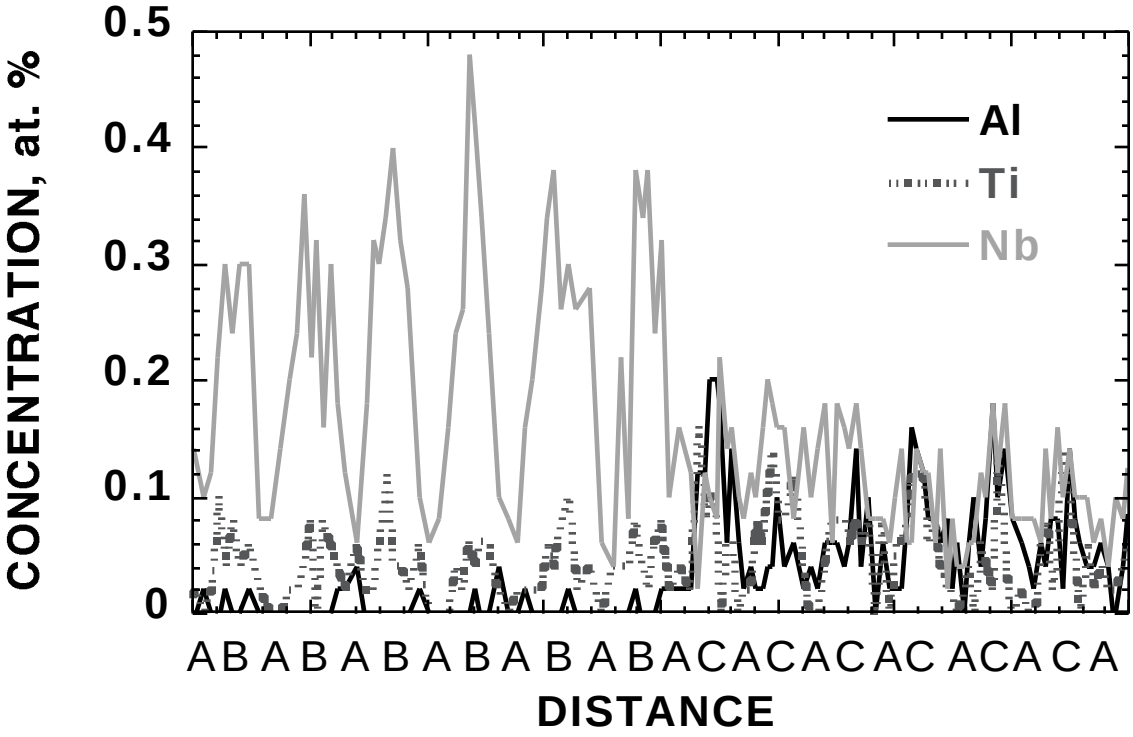

Fig. 5. Composition profile through the central region of a secondary precipitate in Alloy 718